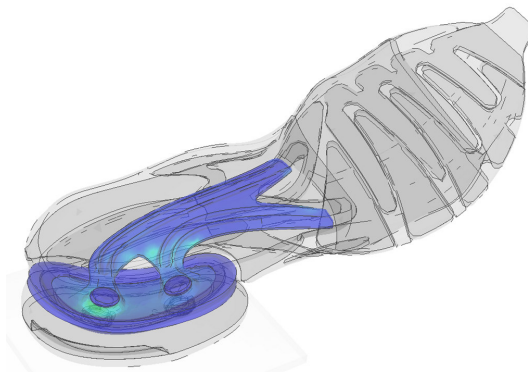


# Advanced Modelling of Sports Footwear



by

**Paul J. Gibbs**

A Doctoral Thesis  
Submitted in Partial Fulfilment of the Requirements  
for award of

Doctor of Philosophy  
of  
Loughborough University

## Chapter 4

# Literature Review: Finite Element Analysis

### 4.1 Introduction

This chapter presents a very brief overview of the finite element method of structural analysis - a subject which can fill many libraries. A short introduction is followed by reviews of the most advanced (and applicable) models in the public domain at the time of writing. It is expected that models of shoes are being created and used by major manufacturers, but the competitive nature of the footwear industry means these models are unlikely to be released into the public domain in the near future (if at all). Modelling of the human foot has been included as most of the work on shoes to date has come out of a need for analysis of medical footwear, almost all of which developed as an extension of a foot model. The final section goes into more detail regarding the use of ABAQUS, the finite element software used in this research.

This chapter does not aim to assess the required accuracy of the various models that will come out of this research, this is to be achieved through physical testing of footwear samples and parts, and is discussed in Chapters 7-9.

### 4.2 The Finite Element Method

Finite element analysis is a theoretical mathematical method of predicting the solution to a physical problem by dividing (discretising) the geometry of the problem into small sections (elements). It is normally used when the precise, analytical solution is too complex to be solved (in the time available), and practical testing is either inefficient or not possible. Each element is analysed using relatively simple mathematics and will normally have a linear or quadratic variation of the desired property with length. The large number of simple calculations required for a FEA solution are suited to processing by computer, and the vast majority of FE analyses are now done in this way (except for teaching purposes, where the problems used are very simple). A major advantage of FE over practical testing is that once a model has been verified (proven to be satisfactorily accurate), there is a high likelihood that the internal stresses in the model are similar to that in the real test situation, allowing the user to probe the inner workings of whatever is being modelled. This can be extremely difficult to do, and sometimes impossible, with real testing.

A FE model is normally constructed from geometry, which is discretised into a mesh; a representation of all the elements in the model, connected by nodes. Each node has a given

number of degrees of freedom (variables in the model). Generally these are the 6 spatial degrees of freedom, but others are available, for example: temperature, conductivity and inertia. External forces, fixings and contact between ‘objects’ are also assigned (known as boundary conditions) to either/both nodes or elements. The elements are assigned mechanical properties (e.g. stiffness) and the problem is then solved in matrix form with appropriate manipulations to give the solution. The size of the matrices directly affects the time taken to process the solution and this in turn is affected by the number of degrees of freedom and complexity of the boundary conditions, as well as of course the processing capabilities of the computer used.

Incorrect specification of any of the material parameters, geometry or boundary conditions, coupled with some unavoidable assumptions that must be made when using the FE technique mean that inaccuracies will be present in the model. It is the job of the FE analyst to be aware of, quantify, minimise and where possible, correct for these inaccuracies.

### 4.3 Material FEA

The first step in creating an accurate model of a midsole is to model the basic materials that it is made of (in this case mostly EVA foam and TPU). If mechanical tests with simple geometry cannot be modelled correctly then a complex full shoe model will be inaccurate, and therefore of limited use, unless the inconsistencies can be assessed and quantified.

A material model is usually created by fitting an equation to test data, the main equation types being linear (e.g. metals in the elastic region), hyperelastic (high strain incompressible materials, e.g. rubber, TPU) and hyperfoam (high strain, highly compressible, e.g. EVA foam). Details on which material models have been used in the shoe models in this thesis are given in Chapter 7.

Material modelling with FEA can be divided into constitutive and macro-scale models, where the former considers the atomic/molecular response of idealised materials, while the latter works on a larger scale overall response. The equations used in constitutive modelling are normally based on the mechanics of the molecular structure, while macro-scale models use curve fitting techniques. Knowledge of how the models work in principle is essential to using them correctly in a model, however this research will only use current material models’ mathematics, and not attempt to develop new equations or fits.

D’Agati (1993) performed linear and non-linear elastic FEA on a simple representation of a midsole, using force input data collected from in-shoe measurements (vertical force only). A single 20-node cube (quadratic) element was used to assess the stress/strain curve, and then this data was used in the midsole model (using the same element type). No numerical results were given, but the paper quotes:

Differences between the linear model’s peak stresses and strains varied from -98% to 680% with respect to the non-linear model’s results.

This is attributed to the non-linear response of the EVA material used.

Swigart (1995) used a vertical impact drop test with an 8.5 kg missile impacting onto ‘midsole specimens’ (the exact nature of these specimens is not specified). Tests results were then applied to an isotropic linear viscoelastic material model and FEA performed. Good correlation was reported for impact heights of 13 & 25 mm, but from 50 mm upwards, the model deviates from the practical results. As an example of this deviation the 50 mm result is shown in Figure 4.1).

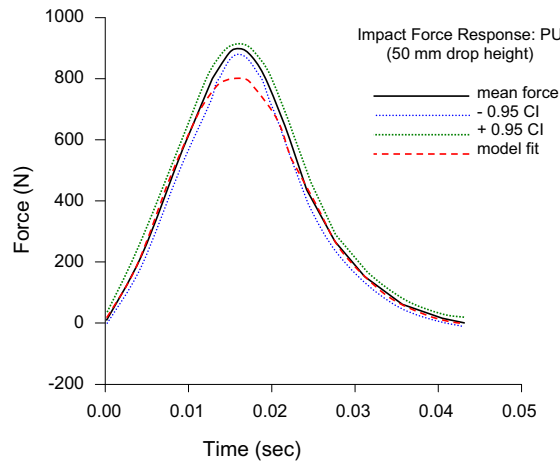


**Figure 4.1:** Drop tests results from 8.5 kg mass falling from 50 mm onto midsole foam; average test values and model predications are shown. Reproduced from Swigart (1995).

Shiang (1997) used FE to study the cushioning response of an unspecified midsole material. Material properties were obtained from compression of a cylindrical specimen under loading by a vertical actuator (Instron machine). Loading values were taken from in-shoe measurements and an assumed shear force of 1/10th of the peak vertical loading was applied to the model (shown in Figure 4.2). Both linear and hyperfoam material models were used, along with different boundary conditions, and models that included combinations of midsole/insole/insole board. It is not clear if the results of the study were verified by comparing real compression of the midsole with the model results.

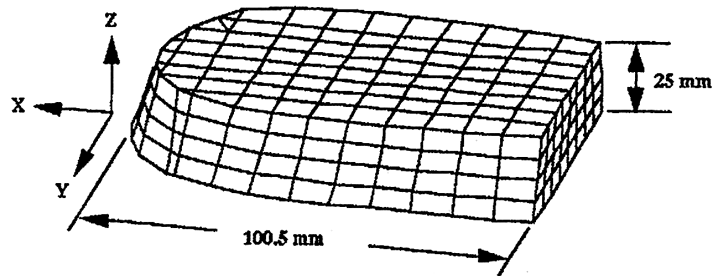


**Figure 4.2:** FE mesh of a simple EVA shoe heel. Shiang (1997).

The response of the foam in car seats was studied by Pajon (1996). Mechanical tests were performed and the test data used to verify the material models. The report notes the importance of verifying the simple material models with complex real parts, as the car seat foam is in a combination of compression and tension and may not be modelled accurately with uniaxial mechanical tests (as can be seen in Figure 3.31).

Thomson (1999) used uni-axial test data to create a hyperfoam material model, and used this to model the heel impact. To reduce processing time, only a cylindrical section of the heel was modelled (this allowed a 2D axisymmetric model, as shown in Figure 4.3). The model was pinned at the base and the nodes on the vertical walls were constrained to move in the vertical direction only. The accuracy of these boundary conditions is questionable and may require practical investigation, although results for this simple model are consistent with the mechanical tests (Figure 4.4).

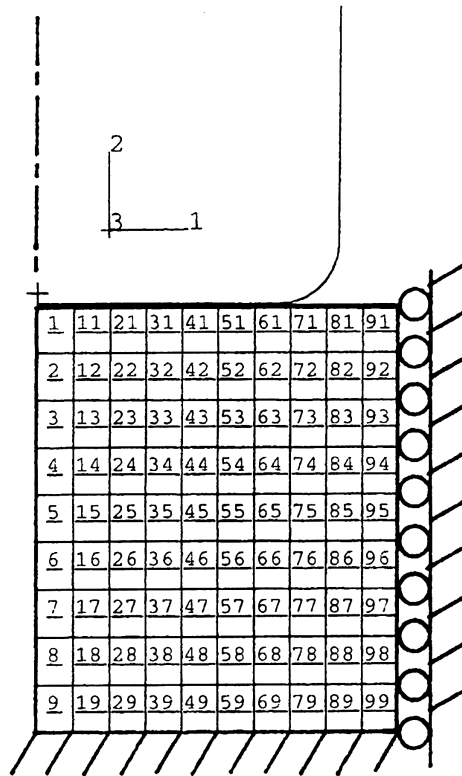


**Figure 4.3:** 2D axisymmetric model of a heel impact (numbers shown correspond to node numbering). Thomson (1999).

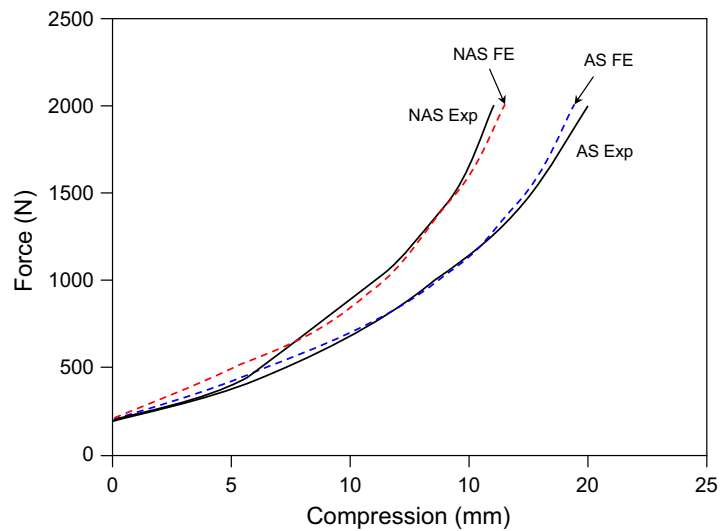


**Figure 4.4:** Experimental and FE results from testing of midsoles that contain (AS) or do not contain (NAS) air pouches. The no-air-pouch model is shown in Figure 4.3. Reproduced from Thomson (1999).

## 4.4 FEA Models of the Foot

Although the forces on the upper surface of the midsole can be measured (Section 2.9), the forces recorded are dependent on the shoe used for the test (as the foot is flexible). Where prototype shoes are available, the forces at the ground/shoe and shoe/foot interfaces can be measured, but the application of these boundary forces to models of entirely new shoes must be carefully considered. To model the forces on the shoe more accurately, some research has gone into modelling the foot. Most of the work aimed at foot-shoe interaction has been concerned with the effect of the heel pad, as this directly affects the peak forces in the heel strike (as discussed in Section 4.5).

Aerts (1993) looked at the effect of various midsoles on the forces transmitted to the leg using human test subjects, but had problems restraining the leg and so the results suffered from inaccuracies. The approach of Noe (1993), although slightly less practical, was more successful. By using fresh human cadaveric lower leg specimens, the bone could be bolted directly to a plate, eliminating any excess vibration. Tests were carried out barefoot and with different midsoles and the report concludes that any evaluation of the shock absorbency of a midsole must take into account their mechanical interaction with the body.

Nakabe (2002) used a moderately complex FEA model of a foot to assess the rotation of the joints during running with a selection of midsoles with stability correction inserts (Figure 4.5). The results were validated with barefoot running and good correlation can be seen for the modelled part of the footstrike (Figure 4.6).

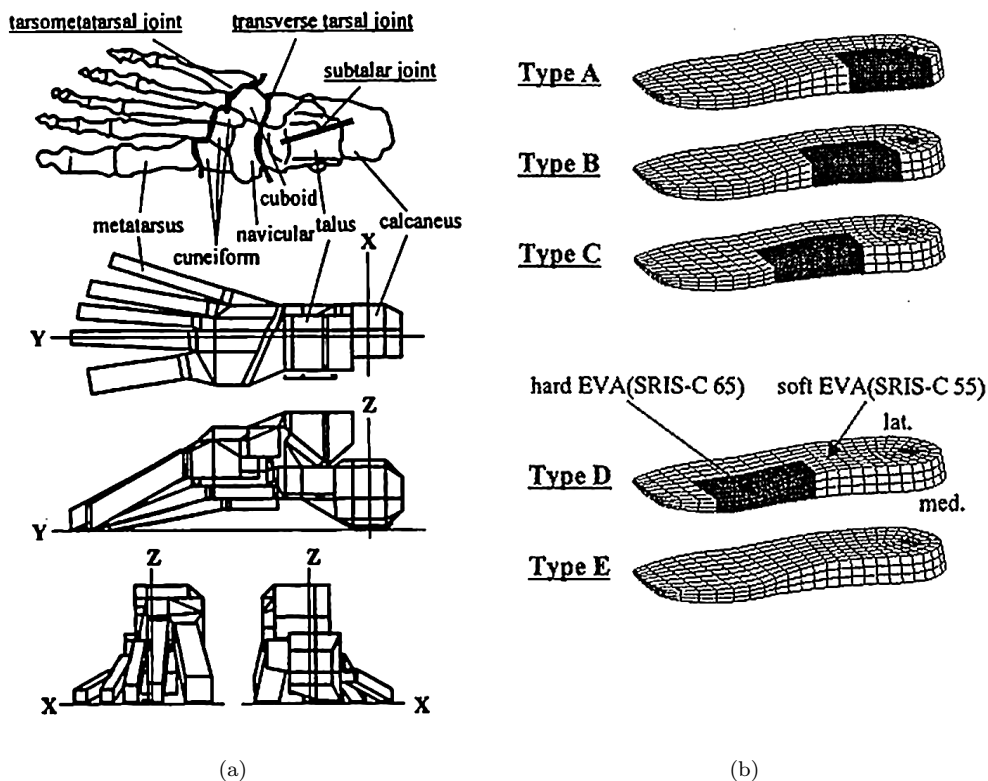


**Figure 4.5:** (a) FEA model of human foot, (b) FEA model of midsoles with stability correction inserts. Nakabe (2002).

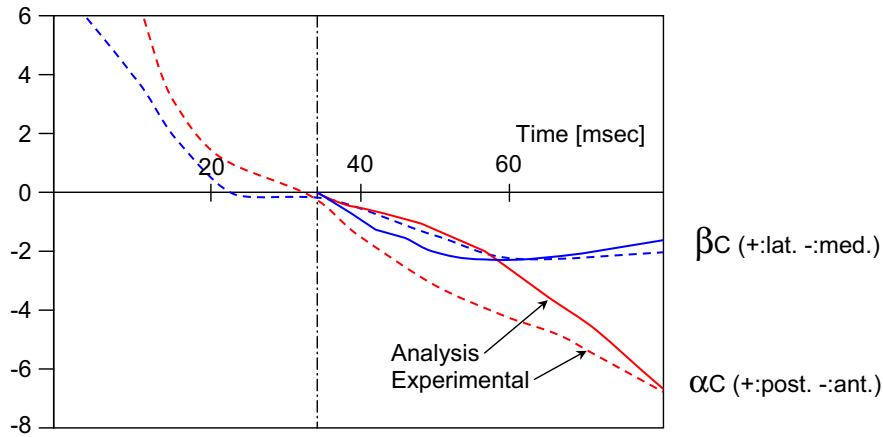


**Figure 4.6:** Results of FEA combined foot/midsole model.  $\alpha_c$  = rotation of the foot plantar-dorsiflexion,  $\beta_c$  = inversion-eversion. Reproduced from Nakabe (2002).

The foot model was progressed by Chen (2003), who modelled the larger bones in the foot and used cable elements to simulate the ligaments. The bones were covered with ‘skin’ to allow the determination of plantar stress distributions on simple midsole surfaces (Figure 4.7). All biological materials were assumed to be linear elastic, the properties are listed in the paper, but the method of determination is not specified.

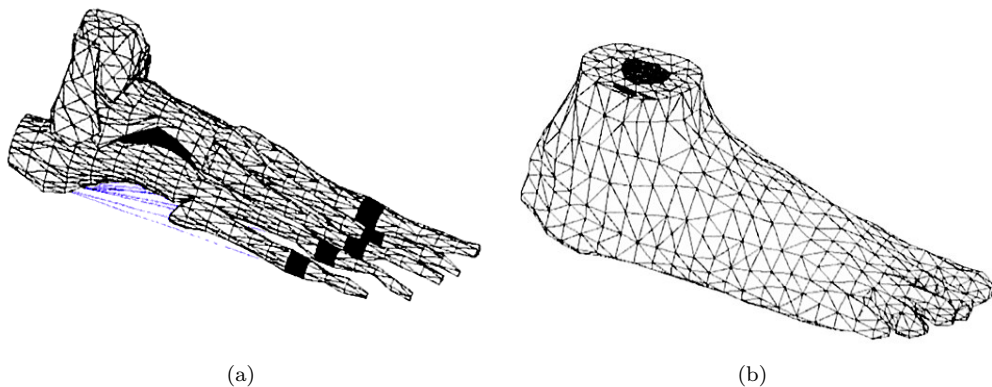


**Figure 4.7:** (a) FEA model of the foot bones with cartilage and major plantar ligaments, (b) complete model of the foot with soft tissues. Chen (2003).

At the time of writing, Cheung (2006) has produced the most realistic foot model. Using images from magnetic resonance scans of a foot, all bones, ligaments and covering flesh are modelled (Figure 4.8). All materials are linear elastic, except the soft tissue and midsole which are modelled as a hyperelastic and hyperfoam material respectively (actual values and sources are given). The paper does not specifically state the verification process used, but in a presentation to the 2006 ABAQUS User’s Conference, the author described experimental loadings of cadaveric foot samples with tendons loaded to simulate various stances. The shoe used in the report is a simple extrusion of hexahedral elements from the flat floor to a surface of a medical insert for a shoe (Figure 4.9).

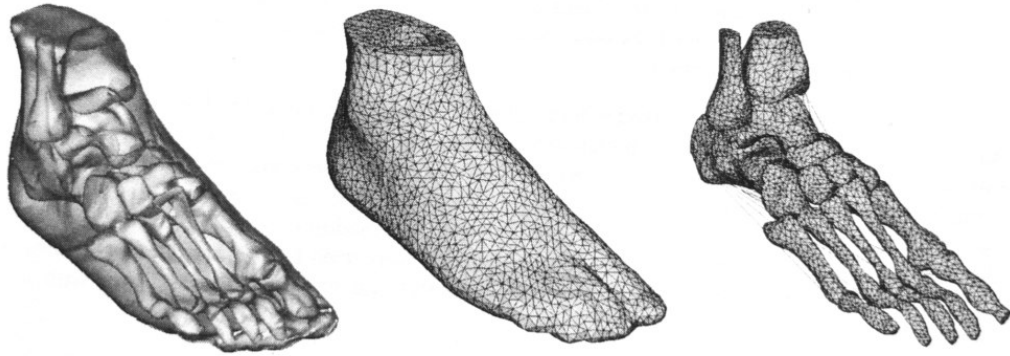


**Figure 4.8:** Left to right: Surface modelled of a MRI scanned foot, FE mesh of encapsulated soft tissue, FE mesh of bony structures. Cheung (2006)

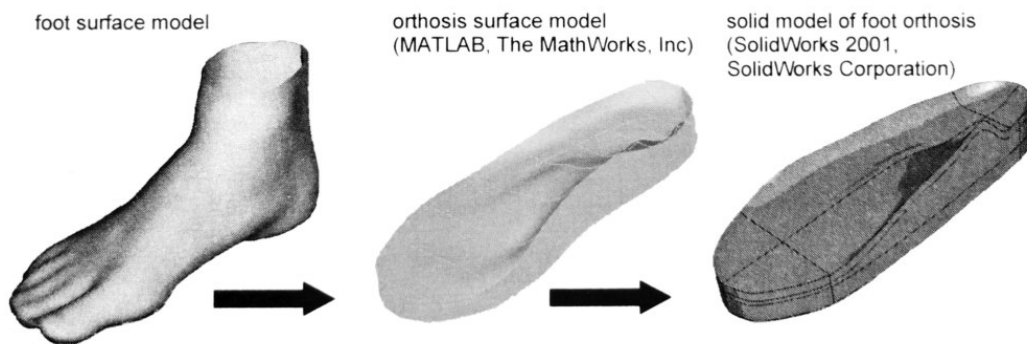


**Figure 4.9:** Procedures for creating the midsole (foot orthosis model). Cheung (2006).



## 4.5 FEA Shoe Models

There is little published research on the use of FEA to model complex 3D shoe models, due to the fact that this approaches the limits of complexity of the available technology and so is likely to be commercially sensitive information (and therefore not being released in full at this time). This section discusses models that have been found in the public domain at present.

A reasonably complex 2D model of a therapeutic shoe was performed by Lewis (2003). The model included some mesh refinement, but assumed all the materials behaved elastically. A static load case was assumed (Figure 4.10). Lewis' results show a difference in the behaviour of the shoe when certain materials are substituted. However, none of the calculations are verified with practical testing.

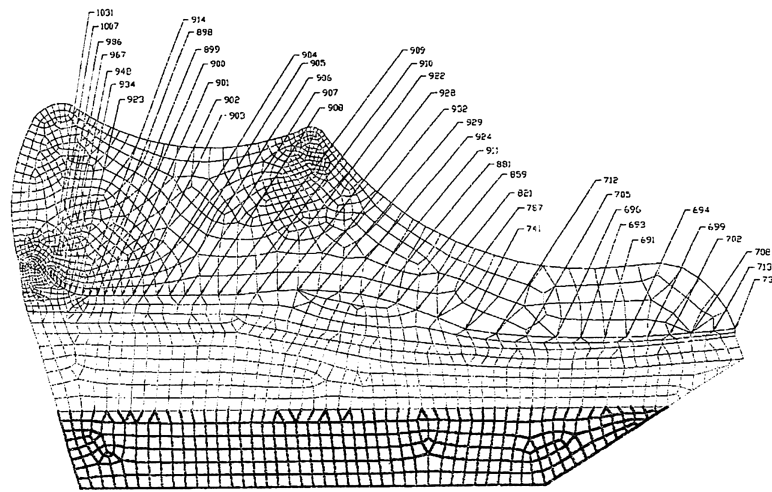


**Figure 4.10:** 2D model of a therapeutic shoe. Numbers indicate nodes of interest in this model. Lewis (2003).

Verdejo (2002) created a similar model to that of Thomson (1999), but with the inclusion of the heel pad. The Ogden hyperfoam material model was used, with data taken from mechanical testing. Model results were verified against ASTM mechanical testing (Figures 4.11-4.12). Verdejo reports that the ASTM testing produces a different pressure distribution on the upper surface of the EVA midsole, compared to that measured in the shoe or predicted by FEA.

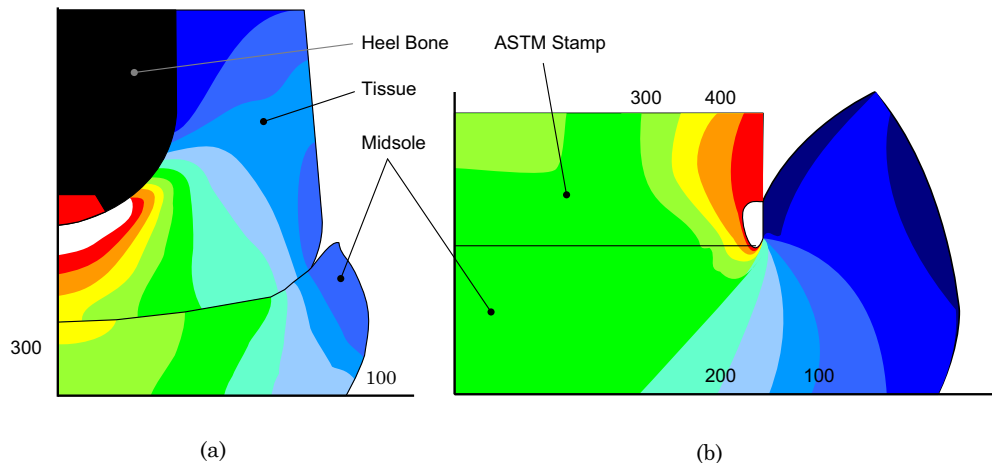


**Figure 4.11:** Contours (kPa) of stress distribution for (a) Heel bone and pad on EVA midsole, (b) ASTM heel on EVA midsole. Reproduced from Verdejo (2002).

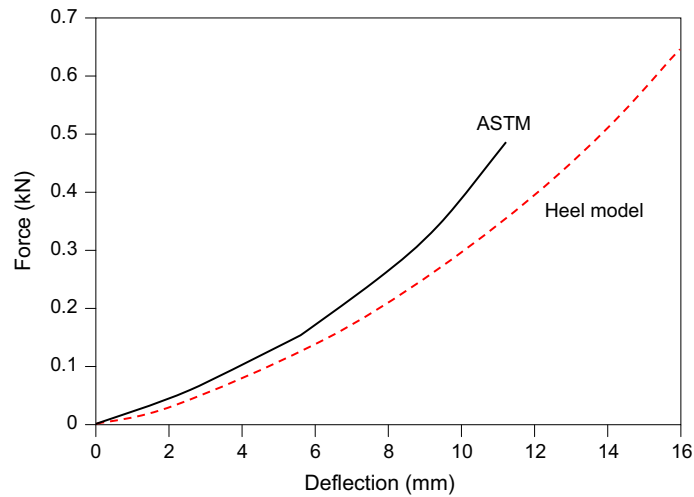


**Figure 4.12:** Comparison of model results and ASTM mechanical testing for model in Figure 4.11(b)). Reproduced from Verdejo (2002).

The only FEA model found to use realistic 3D midsole geometry was found in Nishiwaki (2002). It is shown as a practical implementation of a system for predicting human response to midsoles using human drop tests (see Section 2.9). Very little information is given about the FEA model but the report concludes, “the simulation method is a very powerful tool in the design of shoe soles”. The result of the FEA model is shown in Figure 4.13. Results from an investigation into the effect on cushioning of varying sandwiched EVA layers are also presented in Nishiwaki’s paper.

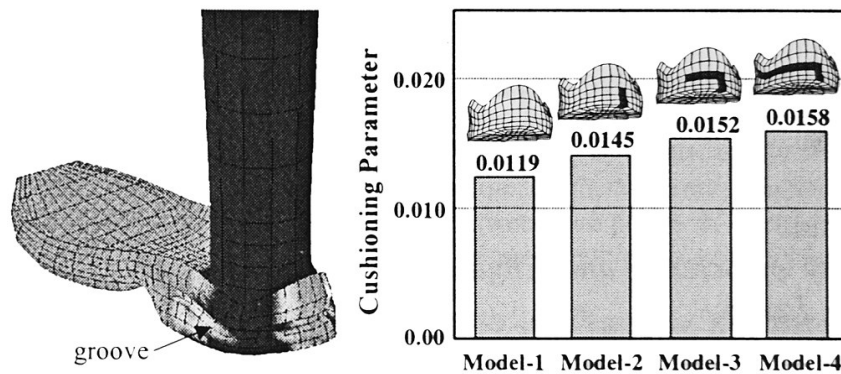


**Figure 4.13:** FEA model of a midsole using realistic component geometry. Black areas indicated on the chart represent areas of reduced stiffness in the model. Nishiwaki (2002).

## 4.6 Modelling in ABAQUS

There are a number of FEA packages available on the market at present. ABAQUS was selected as the solver primarily as it is used by adidas, but it also has a reputation as one of the most accurate mathematical solvers available.

This section will present a concise description of the physical and mathematical principles required to understand the workings of the ABAQUS code. Exhaustive mathematical proofs of all the required matrices and equations are provided in the ABAQUS instruction manuals, so only a few important equations are given here. Where necessary, some wording and quotes have been taken from the various ABAQUS manuals.

The bulk of the materials in the shoes to be modelled are classed as hyperelastic. That is to say that their stress/strain response is non-linear and modelling requires information about this response, ideally, for all strains that are to be modelled. This allows ABAQUS to create the deformation gradient matrix,  $\mathbf{F}$ , as follows:

$$\mathbf{F} = \frac{\partial \mathbf{x}}{\partial \mathbf{X}}$$

where  $\mathbf{X}$  is the initial position of a material particle (for this purpose an integration point on an element) and  $\mathbf{x}$  is its new position. For hyperelastic materials, because the stress/strain response is known over a wide range of strains, the gradient matrix can be calculated. For elastic materials, the assumption that the movement of the point is negligible is made to allow the Cauchy (or ‘true’) stress measure to be used.

To calculate the solution to these matrices ABAQUS comes with two primary solvers; Standard and Explicit. The main difference between these solvers is the way they solve the matrices over time; Standard is implicit - it calculates the value of the result matrix based on the values of the input matrices and the result matrix itself, that is the process is iterative. Explicit, as its name suggests, solves the matrix explicitly; assuming a negligibly small increment between one state and the next, using the result matrix with no further checks. Each of the solvers allows a computational job to be split into steps; separate calculations where the final result of one step forms the initial result of the next. In each step various conditions of the model can be altered.

Standard lends itself to efficient calculation of static and quasi-static problems, but for problems that require the inclusion of inertia, Explicit is better suited. The Explicit solver also has a more robust set of methods for the solution of complex geometry and contact problems and is used almost exclusively in this research for the modelling of shoes. Standard could be used for the modelling of small, simple parts, but the need to predict the behaviour of a part or material sample in the Explicit whole shoe model outweighs the performance advantage of using Standard for such jobs. As an example, the initial modelling of a simple shoe was performed in both Standard and Explicit; a forefoot cushioning test on the Supernova model taking 11.1 minutes in Standard, and 274.5 minutes in Explicit. These jobs modelled the boundary conditions as prescribed constraints, but when ‘physical’ experimental parts such as the stamp and floor were added, the Standard job failed to converge on a solution and had to be abandoned, most likely due to the required increase in contact calculations.

### 4.6.1 Material Models

The equations derived to form the range of material models that are available in ABAQUS are numerous and extensive, so this section will concentrate on the material models selected for use in shoe modelling. These comprise the elastic, hyperelastic and hyperfoam models. The specific forms of these models are known as strain energy potentials.

**Elastic** The elastic material model assumes the stress experienced by an element is directly proportional to its strain. This model has been used where there is little information on material properties, or the material shows an elastic response up to 5% strain and then deforms plastically.

**Hyperelastic** The hyperelastic material model was designed for use with ‘rubber-like materials at finite strains’ and ‘provides a general strain energy potential to describe the material behaviour for nearly incompressible elastomers’. It is a non-linear elasticity model suitable for large (>5%) strains, and is therefore suitable for modelling of shoe components, in particular outsoles and the structures and mechanisms of the new generation of shoes (preliminary modelling showed strains of up to 40% for materials in both EVA and structure components in simple shoes). The hyperelastic model assumes isotropy for the following reasons:

The initial orientation of the long-chain molecules in elastomeric materials is assumed to be random - therefore the material is initially isotropic. As the material is stretched, the molecules orient themselves, giving rise to anisotropy. However, the development of this anisotropy follows the direction of straining - hence, the material can be considered to be isotropic throughout the deformation history. As a consequence, the strain energy potential can be formulated as a function of the strain invariants.

The strain energy potential defines the strain energy stored in the material per unit of reference volume (volume in the original configuration) as a function of the strain at that point in the material. ABAQUS provides a number of different forms of strain energy potential to model the approximately incompressible elastomers, including: Arruda-Boyce, Mooney-Rivlin, neo-Hookean, Ogden and Yeoh forms. Some of these are derived from purely polynomial curve fitting, while others are phenomenological - they are based on extrapolations of the underlying cellular/molecular structure of the material. The exception is the Marlow form, which is designed to fit any test data to a fairly smooth non-polynomial curve. The choice of a particular form should be based primarily on verified model results.

All the energy potential forms require some kind of sample data to formulate their coefficients, the most basic requirement being uni-axial tests (see Section 3.4). The uni-axial data only specifies the material property in one compression/tension mode, so assumptions are made about the other modes unless extra test data from bi-axial and tri-axial experiments are included. The use of tri-axial data is recommended when the material being modelled is compressible. Once data has been inputted, ABAQUS calculates the required energy potential form coefficients and allows the user to compare results for a given range of strain - useful for checking if any of the forms becomes unstable in the expected range of strain.

**Hyperfoam** The ABAQUS hyperfoam model is similar to that of the hyperelastic model, but it accounts for the difference in deformation modes in compression and tension exhibited by most elastomeric foams (see Section 3.3.1). The model is designed for materials that can deform elastically to large strains, including up to 90% in compression. Isotropy is assumed.

## 4.6.2 Material Model Modifications

In addition to a non-linear elastic stress-strain response, shoe materials (especially foams) can contain a number of energy-loss mechanisms (as discussed in Section 3.3). The resulting overall response of the material is vital for providing the correct performance during a running strike and so any computer model that attempts to simulate the entire footstrike accurately must contain representations of these mechanisms.

### 4.6.2.1 Hysteresis and Viscoelasticity

A repeatable change in the stress-strain response between the loading and unloading cycle, and the resulting energy loss, can be modelled either with the \*HYSTERESIS or \*VISCOELASTIC functions within ABAQUS. Both models take a defined stress-strain response and modify it with relation to the strain rate the material experiences. The main difference between the two models is that \*HYSTERESIS can only be used with large-strain hyperelastic models, not hyperfoams, due to the model assuming no strain-rate dependence with a change in volume, but only in shear. The viscoelasticity model allows a range of inputs, including specification of the strain-rate response using a Prony series, normally obtained from multiple creep tests, or DMA (Dynamic Measurement Analysis) which provides a much faster physical test and is described in detail in Section 5.2.4.2.

### 4.6.2.2 Mullins Effect

As discussed in depth in Section 3.3.3, the Mullins effect provides a way of dissipating energy from the model via permanent deformation of the material. It is strain and strain-history dependant. To incorporate this damage into the material model, ABAQUS uses a damage calculation that removes a given amount of strain energy upon loading of the material. This can be expressed:

$$U_{Total} = (U_{stored} + U_{lost})_{Deviatoric} + (U_{stored} + U_{lost})_{Volumetric}$$

When used with \*HYPERELASTIC, the \*MULLINS EFFECT calculation assumes that only the deviatoric strain is subject to loss. When using \*HYPERFOAM, damage occurs on both deviatoric and volumetric strain.

The variables for the damage model can be inputted directly, or derived from multiple strain-level cyclic test data by way of a least squares fit, as is done for specifying the primary behaviour via \*HYPERELASTIC or \*HYPERFOAM. However, the ABAQUS documentation does strongly recommend that the resulting fitted coefficients are verified by single-element models against the test data.

### 4.6.2.3 Combining Material Model Modifications

The materials used in shoes are subject to hysteresis, viscoelasticity and the Mullins effect. Unfortunately, these energy loss mechanisms are currently incompatible within ABAQUS; \*MULLINS EFFECT cannot be used in conjunction with \*VISCOELASTIC or \*HYSTERESIS. Even if the material data are collected from samples pre-strained to the average maximum strain seen in use, this data will be too stiff or too soft for the majority of the material. This is not so much of a problem in simple geometry shoes where the strain is fairly constant, but it is a major issue in structure shoes. As the Mullins effect can greatly reduce the stiffness of a section of material, there is a real risk of under-prediction of stress in a component that could result in material failure. While the material model could be created from pre-stressed material data, this will only predict correct stresses in simple, homogenously strained parts.

Components with highly varying strain fields (such as the Ultraride structure plate under a heel stamp test, Figure 4.14), will not have their stress predicted correctly using a single material curve.

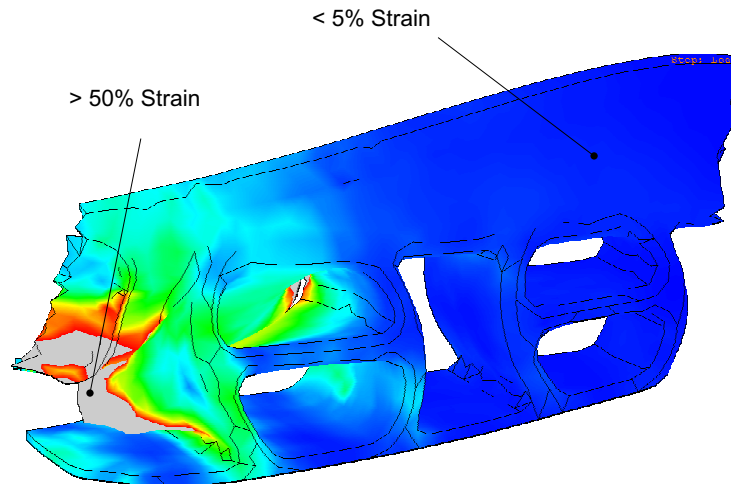


**Figure 4.14:** Strain result from a heel stamp test performed on the structure plate of the Ultraride, showing a large range of strains occurring in the same part.

Recent work by Bergström (2006a) has produced a phenomenological material model that extends the functionality of the ABAQUS \*HYSTERESIS command to incorporate the Mullins effect and include rate-dependency. This model was not available during the research for this thesis, but it has the potential to be very useful for future work.

A less practical method of including rate-dependency and the Mullins effect is described in Section 8.5, where a model is run using \*VISCOELASTIC and the results analysed for strain levels and the material model adjusted accordingly for the next iteration. This method has two main drawbacks; the material models are discrete and each iteration requires a complete re-run of the analysis, extending development time.

#### 4.6.2.4 Bulk Viscosity

If neither viscoelasticity, hysteresis nor Mullins effect is specified, a material in a dynamic, temperature independent, elastic model has no method of dissipating energy which can result in unstable models. To this end ABAQUS applies an energy loss mechanism known as *bulk viscosity* to reduce the likelihood of elements under high strain-rates collapsing in Explicit. The application of bulk viscosity is discussed in Section 4.6.4.2.

#### 4.6.3 Element Performance and Selection

Various element types are available in ABAQUS, but this section will pay attention only to those to be used in the modelling of shoes: three dimensional tetrahedral and hexahedral. The basic elements, C3D4 and C3D8 are shown in Figure 4.15. Across each face, and between the faces, lines of integration exist where the properties and response of the element are calculated during the analysis. The more integration points and lines an element contains, the more detailed the changes in property across the element can be modelled.

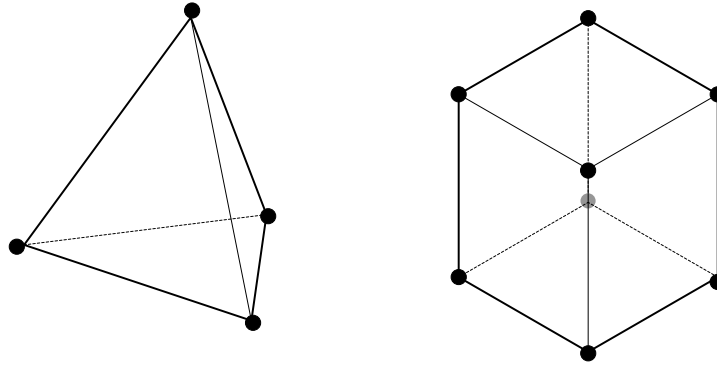


**Figure 4.15:** 4-node tetrahedral (C3D4) and 8-node hexahedral (C3D8) elements

These are the most mathematically simplistic of the 3D solid elements, and as such are the most computationally efficient. These elements cannot be used in all circumstances however. For example, the linear C3D8 element will become ‘shear locked’ when used in a direct bending model (Figure 4.16). The linear hexahedral element begins the step as shape (a). In the physical solution the element should become (b), but as the element formulation has a constant strain, the integration lines (dashed) must remain of equal length and the sides of the linear element cannot bend, generating large shear stresses (c), resulting in a stiffness modulus that approaches infinity.

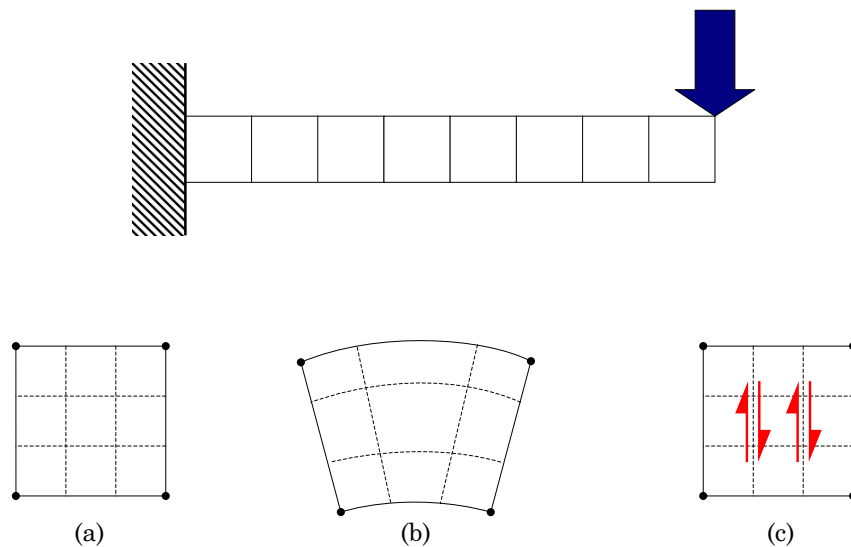


**Figure 4.16:** Linear hydrostatic elements in a simple bending model (top). (Note: For simplification of the diagram, only 2D elements are shown, but the principles also apply to the 3D).

To overcome this problem the element must be substituted for the quadratic version (C3D10 and C3D20, Figure 4.17), which allows a variation in strain, or have its integration modes reduced (C3D8R) giving a single deformation gradient across each face. A fine mesh of reduced elements arranged in layers more than one element thick is recommended for meshes that are likely to see high distortion.

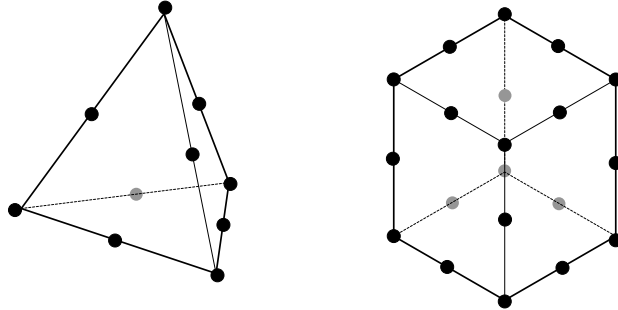


**Figure 4.17:** 10-node tetrahedral (C3D10) and 20-node hexahedral (C3D20) elements

Reduced integration elements can however exhibit hourglassing modes (Figure 4.18) where the stiffness of the element is effectively zero as a change in the shape of the element does not always result in a change in the length, or relative angle, of the integration lines.

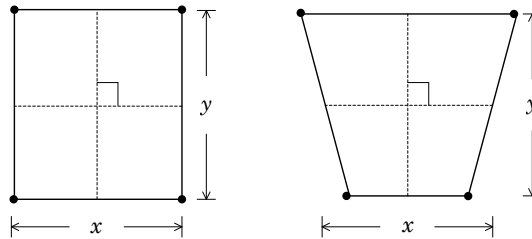


**Figure 4.18:** An element exhibiting an hourglassing mode. Note the change in shape of the element with no change in the deformation gradients.

To combat this behaviour, a number of controls are available to modify the behaviour of the element. The default control in Explicit is ‘Viscoelastic’, where the rate of volume change of the element is artificially damped at the start of a step, after which control is based on the stiffness response of the material. This initially stops the hourglassing, but assumes that the maximum load change will occur at the beginning of the step, which is not always the case.

This problem can be overcome by using the ‘Enhanced’ hourglassing control, which combines a stiffness based and viscoelastic based control of the deformation throughout the step. This results in a small decrease in element efficiency, but is vital for some jobs to run with realistic results (the use of a purely viscoelastic control, while more efficient, can result in severe hourglassing in quasi-static conditions during a step).

Another method of avoiding the shear locking problem is the use of incompatible mode elements (C3D8I, Figure 4.19). Additional integration modes are added on the diagonals of the element to control the trapezoidal distortion associated with locking.

In general all elements produce more accurate results the closer to their ideal shape they are (e.g. square faces at  $90^\circ$  for hexahedral elements). Generally tetrahedral elements have lower sensitivity to distortion so are recommended for meshes undergoing high strains, though



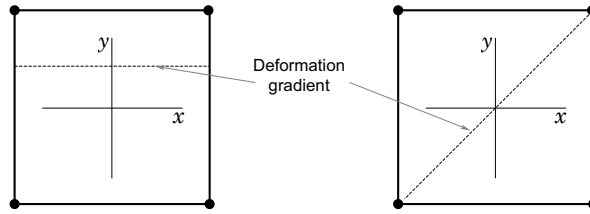


**Figure 4.19:** Face of a C3D8 element with normal (left) and incompatible (right) density gradient modes.

the increased numbers required to fill the same volume will create a slower running job.

The modelling of incompressible substances (where the Poisson's ratio,  $\nu$ , of the material is close to 0.5), can give rise to problems due to round off errors, as the stress increase for a given deformation approaches infinity as  $\nu$  approaches 0.5. To avoid this, hybrid elements are offered that calculate the pressure stress and displacement stiffness as separate, but coupled, variables.

#### 4.6.4 Job Controls

It is often the case that a more accurate finite element model requires the addition of more physical processes into the calculations with a resulting increase in the time taken to process. Although performance of easily available desktop computers is increasing at a steady rate, there still may be a need to reduce the time taken to achieve a useful result from FEA. These controls are discussed here in theory and in Section 8.4.2 with relation to practical application.

##### 4.6.4.1 DOF Reduction

The most obvious way of reducing the processing time of a job is to reduce the amount of calculations required. This can be achieved by reducing the number of degrees of freedom (DOF) in the model. Replacing quadratic elements with linear ones is a quick method of achieving this (provided any interactions or boundary conditions are specified on an element basis), though there is a notable performance difference between some types of elements, as discussed in Section 4.6.3.

If a reduction in accuracy is acceptable, then physical processes can also be removed (such as viscoelasticity). However, if removing these process destabilises the model, causing vibration and extra movement, the number of iterations a job needs can increase, having the reverse effect and slowing the overall job time down.

If parts of the model have a negligible effect on the current test, then they can be removed or substituted. For example, if the interest is in the performance of a heel part under heel cushioning, then the forefoot of the model could be meshed coarsely, or removed entirely. This can give significant reductions in job times, but the effects on the results should be checked.

##### 4.6.4.2 Mass Scaling

As discussed at the start of this section, for simple problems ABAQUS/Standard is a very fast solver, but it drastically loses efficiency as the models increase in complexity, and in some contact models cannot provide a solution. To provide faster solutions using ABAQUS/Explicit,

a number of solution controls are used, the most powerful (and complex) of these being mass scaling.

The total time a job will take to process is roughly dependant on the number of degrees of freedom to be solved in each increment and the number of increments to be solved. The solver automatically limits the size of the time increment based on the global stable time ( $\Delta t$ ) of the model. Fundamentally this is a measure of the shortest time it takes a stress wave to propagate across any of the elements, this is based on factors including stiffness, size and damping, following the equation:

$$\Delta t = \min \left( L_e \sqrt{\frac{\rho}{\hat{\lambda} + 2\hat{\mu}}} \right) \quad (4.1)$$

where  $L_e$  is the characteristic length of an element (in an undamped material this is the length of the shortest side),  $\rho$  is the density and  $\hat{\lambda}$  and  $\hat{\mu}$  are the effective Lamé's constants, which are derived:

$$\hat{\lambda} = \lambda_0 = \frac{\nu E}{(1 + \nu)(1 - 2\nu)}$$

$$\hat{\mu} = \mu_0 = \frac{E}{2(1 + \nu)}$$

where  $\nu$  is Poisson's ratio and  $E$  the Young's modulus of the material (ABAQUS Analysis User Manual 6.3.3).

As a result of this, any model with unrealistic, super light or stiff materials will produce a very small time increment. Elements with super light or soft properties are likely to be deformed and crushed, also producing a short wave speed and thus a small time increment.

However, using mass scaling, the time increment can be controlled by varying the density of the material with values selected to either fit to a user-specified time increment or level of scaling. The level of scaling is specified as a multiple and reported as a percentage increase in overall mass. Mass scaling is excluded from gravitational calculations, so the extra mass cannot be "weighed" in the model, it only causes an effect through a change in inertia (ABAQUS Analysis User Manual 7.6.1).

The automatic controls can be overridden in a number of ways, ranging from specifying a set increment (for example in jobs involving only rigid bodies), to giving merely a start value and allowing the solver to adjust values throughout the job. This can decrease job time by orders of magnitude, but can affect the output significantly, and may cause job failure or non-physical results. While the ABAQUS manual recommends limiting the mass increase to around 2%, useful qualitative results have been achieved with scalings of up to 1,000,000%, corresponding to a reduction in job time of around 1000 times (see Section 10.4). While this contradicts the advice against using super-stiff materials, with shoe modelling the scaling is applied mostly to the steel impactors, which undergo very small deformations and if their movement is specified by position, then the extra mass has a negligible effect on the result.

Mass scaling is automatically applied to all Explicit jobs in the form of bulk viscosity. By adjusting the density of the material slightly, a similar effect to that of the element floating in a viscous fluid is achieved - this is very similar to directly applied mass scaling, but on a much smaller scale. Bulk viscosity ( $\rho_{bv}$ ) is calculated thus:

$$\rho_{bv} = (bL_e \dot{\epsilon}_{vol})^2 \quad (4.2)$$

where  $b$  is the inputted co-efficient and  $\dot{\epsilon}_{vol}$  the volumetric strain rate. The automatically-

calculated bulk viscosity has been found to be ineffective in most of the shoe models, as the time increments are quite large to begin with.

**Fixed Time Increment** Generally it is best to allow ABAQUS to calculate the time increment in an Explicit job automatically; this allows the time increment to reduce in response to very small elements, but also to increase when the computation becomes less demanding. However, during some models where there are stiff parts that undergo little strain (such as drop tests), the part can be made rigid (either as a new rigid part, or using \*RIGID) and mass scaling can be applied to all of the model *excluding* that part. Using the fixed time increment ‘drives’ the job along at a constant rate, ignoring the limitations of the stiff elements in the rigid part. This method can give very fast processing jobs, but will fail if there is moderate to severe mesh distortion anywhere within the model.

### 4.6.5 Contact

Contact in FE models should occur when two or more objects collide. However, objects will occupy the same physical space without having an effect on each other unless a specific contact interaction has been defined between two or more surfaces (external parts of objects), which must also be pre-defined. ABAQUS allows surfaces to be specified as node-based, element-based or analytical rigid. Node based surfaces are non-continuous as nodes are intersections of element edges and are mathematically considered discrete. Element surfaces are continuous, and contain more information about a given surface as the curvature and area of each element is known - this allows more accurate calculation of the transfer of forces between two element based surfaces and leads to much better results for contact problems. Analytical rigid surfaces are a special case as they are described using straight and curved line sections, either rotated or swept to form simple shapes. They allow much better definition of curved surfaces (as they are not discretised), but their use has restrictions.

Contact between one node-based surface and another, or contact with itself, is not permitted in ABAQUS, the same is true for analytical rigid surfaces. Element-based surfaces are allowed to interact relatively freely. Each interaction requires a definition of the interaction and an algorithm for calculating the result.

#### 4.6.5.1 Interaction Definition

Contact is a large set of complex mathematical descriptions and is treated differently within Explicit and Standard. As Explicit is used in the vast majority of the models created in this research, only this is discussed (in brief) here. Full details of all the theory and formulations is found in the ABAQUS Analysis User Manual 21.1.1.

There are two methods available for defining contact between surfaces in Explicit: general contact and contact pairs. General contact sets up every element in the model as a single surface and allows this master surface to contact itself. The contact pair method requires the User to specify a pair of surfaces. The advantages of each method are summarised:

#### **General Contact**

- A single surface can span multiple objects.
- A surface can have both rigid and deformable regions.
- A surface can have solid and shell elements.
- Nodes can have contact with more than one surface at a time (very useful for modelling objects with corners).

- T-junctions of shell elements can be modelled with one surface.
- Changes can be made to surface descriptions between modelling steps.
- General contact has a built-in surface smoothing algorithm for element based surfaces.

Each of the functions above are not available when using contact pairs. Conversely, the following functions are only available with contact pairs:

#### **Contact Pair**

- 2D surfaces can be defined.
- Analytical rigid surfaces can be defined.
- Thermal contact can be defined.

The limitations on each method are reduced with each new version of ABAQUS, for example, both methods have to be used in shoe models as the structures have too many surfaces to define as pairs, but the floor is usually modelled as an analytical rigid body, requiring a contact pair (the latter limitation is to be removed in ABAQUS version 6.6).

The default setting for the contact algorithms are also different; general contact uses the penalty enforcement algorithm while contact pair uses kinematic.

#### **4.6.5.2 Contact Algorithms**

ABAQUS includes two main methods for processing surface contact; small-sliding and finite-sliding. Small-sliding assumes a negligibly small displacement of one surface along another and does not allow separations after contact, but is much more computationally efficient. Finite-sliding allows any finite movement of the two surfaces, including separations, with a reduction in efficiency. To correctly model any interactions between surfaces in shoes the finite-sliding method must be used as separation can occur after contact.

The Explicit solver provides many options for the algorithms that deal with the finite-sliding motion, but the main choice in job set-up is the use of kinematic or penalty contact enforcement:

**Kinematic** For each time increment the kinematic algorithm will first displace nodes, then calculate the pressure increase generated by the penetration of one surface into the other (a non-physical condition). Corrections are then made to satisfy the pressure balance (but not necessarily the penetration). The sub-options of ‘hard’ and ‘soft’ contact can also be specified (ABAQUS Analysis User’s Manual: 22.1.2), where hard contact transmits forces between surfaces with zero distance between them. Soft contact gives a linear relationship between the percentage of the force transmitted and the distance between the surfaces (this can be a positive or negative distance). Hard contact is designed to reduce the penetration of the surfaces, but the level of final penetration depends heavily on the quality of refinement of the mesh. Hard contact can leave small gaps between contacting surfaces as the kinematic algorithm disregards the inertia of the nodes on the contacting surfaces (hence they can ‘bounce back’ off the surface).

**Penalty** Penalty contact will first look for penetrations in the current configuration, then apply deformations to remove that penetration. These deformations are generated by introducing artificial stiffness increases into the slave nodes. To this end, penalty contact treats the penetration of surfaces more accurately, but the pressure distribution becomes less accurate. This increase in stiffness also has a detrimental effect on the stable time increment

(slowing down the job), although the stiffness values are chosen automatically to balance the accuracy of contact with the increment time. The use of hard contact also reduces penetration, but while there is likely to be less penetration than using kinematic, the penalty algorithm does not guarantee there will be no penetration. The penalty algorithm accounts for all the energy during contact, so the inertia of the contacting nodes is retained (useful for jobs where rebound is likely).

Both algorithms can have problems resolving contact between surfaces of significantly different masses, due to high velocities being generated in the lighter material in an attempt to conserve overall energy across the contact. In Figure 4.20(a) a less dense master surface has a high velocity of contact and penetrates the slave surface in the next increment (b). The algorithm then resolves the contact based on the slave surface deforming and providing a pressure that moves the master surface back slightly (c).

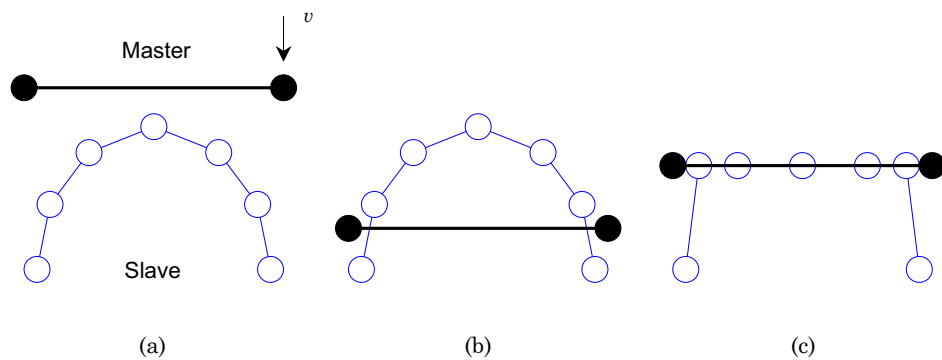


**Figure 4.20:** Surface contact errors due to mismatched material densities.

To overcome this problem, the master surface should be specified as the coarser, denser mesh. If this is not possible then the priority balance between master and slave surfaces can be manually over-ridden. If the default value of 1.0 gives surface ‘A’ as the master, then changing the priority to 0.0 gives surface ‘B’ as the master. Any value between 1.0 and 0.0 requires a weighted average of the results, with 0.5 giving a result generated from one calculation with A as master, and one with B as master. This method gives the most accurate results, but is the most computationally intensive.

#### 4.6.6 Connectors

For the efficient modelling of mechanisms, ABAQUS provides a set of specialist connector elements. These act as packaged boundary constraints, specifying a particular linked relationship between two nodes in the model.

While the aim of the connector elements is to provide a quick method of simulating joints etc., they have proven to be unreliable in models with complex geometry. They are very sensitive to overconstraints; where a single degree of freedom is constrained more than once. As overconstraints can be formed from a change in contact conditions throughout the job, the use of connectors requires very careful job set-up, and if a job fails, lengthy debugging and adjustments to the model are needed to allow successful execution (see Chapter 9).

## 4.7 Chapter Summary

This chapter has reviewed the state of knowledge of finite element analysis, applied to a footwear modelling application. It is apparent that there is a good depth of knowledge in the mathematical modelling of hyperelastic materials, however the application of these models into FEA has been limited to more traditional industrial applications. Specific modelling of footwear has been concentrated on the biomechanical or medical (orthopedic) use of models, with complex foot assemblies but only very simple midsoles.

Looking at the techniques offered in one of the most popular FE programs, ABAQUS, shows that the technology is available to model the materials, geometry and interactions involved in footwear. Simple models have given reasonable results in the past and the application of FE mechanism modelling used in other engineering areas should allow the modelling of the increasingly complex modern shoes.

It must be noted that while there is a range of data available for the biomechanical inputs into the system and some general data on material properties, there is no apparent quantifiable information detailing the variation between one shoe and another of the same size, make and model. This information is lacking both in the public domain and within adidas.

The literature review in Chapters 2-4 proves that the methods proposed in this research will provide new insights and fill in vital gaps in knowledge in this field:

- FEA modelling of simple and complex running shoes.
- Laboratory determination of the properties of the materials in said shoes.
- Material model validation with FEA.
- Shoe model validation using practical mechanical testing.
- Determination of the overall variability of the shoes modelled.

With enough time, this kind of analysis should be possible, but for it to be applicable to industry it must be able to be carried out within a production time scale (e.g. a few weeks) with little manpower resources. The following issues are believed to be critical in achieving the correct speed/accuracy balance for the FEA models:

- The level of model complexity, specifically mesh densities, use of component bonds, contact and complex material behaviour such as Mullins effect and viscoelasticity.
- The level of accuracy of geometry required to produce adequate meshes (as the geometry may need repair, as discussed in Chapter 8).
- The sensitivity of the model to slight changes in any of the aforementioned model parameters and geometry.
- The level of repeatability of performance of manufactured shoes.

Investigations into all of the above are carried out in Chapters 7-11 to address these questions. The use of FE models within a production time scale, along with suggested workflows is discussed in Section 12.5.1.